Barotropic Tides in the Northeast Atlantic Inferred from Moored Current Meter Data

Gerhard Dick and Gerold Siedler

UDC 551.466.75; Northeast Atlantic

Summary

Current data obtained from 7 moorings in the Northeast Atlantic in the course of many years are analysed with respect to semi-diurnal barotropic and baroclinic tides and diurnal barotropic tides. For semi-diurnal tides M_2 and S_2 the energy distribution is usually dominated by the barotropic mode; only in a few cases does the first-order baroclinic mode contain higher energy. Barotropic tidal ellipse orientations are found to be consistent with results from earlier tide gauge observations in this area. Significant deviations occur, however, in amplitudes. Results for the diurnal component K_1 are also presented. With few exceptions, tides are found to be progressive waves in this area. The current ellipse pattern is similar to results obtained indirectly by Cartwright, Edden, Spencer et al. [1980] from tide gauge observations.

Barotrope Gezeiten im Nordostatlantik aus Daten verankerter Strömungsmeßgeräte (Zusammenfassung)

Strömungsdaten von 7 Verankerungen, die im nordöstlichen Atlantik über mehrere Jahre ausgelegt waren, wurden im Hinblick auf halbtägige barotrope und barokline sowie eintägige barotrope Gezeiten analysiert. Bei den halbtägigen Tiden M_2 und S_2 dominiert normalerweise die Energie der barotropen Eigenfunktion, nur in wenigen Fällen enthält die barokline Welle 1. Ordnung höhere Energie. Die Ellipsenorientierungen für die barotropen Komponenten entsprechen früheren Ergebnissen von Tiefseepegeln in diesem Gebiet. Es gibt jedoch signifikante Abweichungen bei den Amplituden. Die Gezeiten in diesem Gebiet sind fast ausschließlich fortschreitende Wellen, in einigen wenigen Fällen jedoch vom gemischten Typ. Die räumliche Änderung der Strömungsellipsen entspricht weitgehend den Ergebnissen, die Cartwright, Edden, Spencer et al. [1980] indirekt aus Pegelbeobachtungen erhielten.

Les marées barotropes dans l'Atlantique Nord-Est, déduites de mesures effectuées à l'aide de courantomètres mouillés (Résumé)

Les mesures de courants provenant de 7 mouillages sur plusieurs années en Atlantique Nord-Est ont été analysées en ce qui concerne les marées semi-diurnes barotropes et baroclines et les marées diurnes barotropes. Pour les marées semi-diurnes M_2 et S_2 la répartition de l'énergie est généralement dominée par le mode barotrope; dans peu de cas seulement, le mode barocline de premier ordre renferme la plus haute énergie. Les orientations de l'ellipse relevant de la marée barotrope sont en accord avec les résultats d'observations marégraphiques antérieures dans cette région. Des écarts significatifs apparaissent toutefois en amplitude. Les résultats

concernant la composante K_1 sont également présentés. A quelques exceptions près, les marées, dans cette région, se sont trouvées être des ondes progressives. Le type d'ellipse des courants est semblable aux résultats obtenus indirectement par Cartwright, Edden, Spencer et al. [1980] à partir des observations marégraphiques.

1 Introduction

The advances in the numerical modelling of ocean tides (Hendershott [1977, 1981]; Accad and Pekeris [1978]) have increased the need for precise measurements of open ocean tides, particularly in regions of rough topography, in order to check and improve the established models (Schwiderski [1980]). With the advent of deep-sea pressure gauges open-ocean sea level data became available (Unesco [1975]; Cartwright et al. [1980]; Baker [1981]). The growing number of long-term current meter moorings deployed in some parts of the ocean now provide an additional data base, providing information on barotropic and baroclinic tidal currents.

In the eastern North Atlantic, Cartwright et al. [1980] obtained deep-sea tide gauge data at selected positions on lines from southern Portugal to the Azores and from there to Iceland and then to Scotland, on a line from the Mid-Atlantic Ridge along 54° N towards Ireland and also along the shelf edge west of Ireland and the British Isles. The "response" method of Munk and Cartwright [1966] was used for the analysis. Boundary data were interpolated by hand-drawing smooth cotidal curves, and barotropic tidal currents were deduced from the pressure gradients in the resulting cotidal maps. Direct observations of tidal currents in this area near the continental margin were presented by Gould and McKee [1973] and Meincke, Siedler and Zenk [1975] and for one site in the Madeira Abyssal Plain by Saunders [1983]. For tidal currents in the surrounding area we refer to Regal and Wunsch [1973] and Schott [1977].

In the present study current meter data from moorings in the eastern North Atlantic were analysed with respect to the dominating semi-diurnal and diurnal tides. The tidal currents thus obtained are compared to the currents deduced from pressure-gauge data by Cartwright et al. [1980] and to Saunders' [1983] moored current meter results from one site in the southern part of the area under discussion. Thus new current data are presented, and indirectly deduced tidal current properties are checked in an attempt to provide an extended data base in the eastern North Atlantic for the verification of numerical tidal models.

2 The data set

The current meter data used in this analysis were from moorings of the international Northeast Atlantic Dynamics Study (NEADS) and also from moorings deployed in the region by the Institut für Meereskunde an der Universität Kiel (Dickson [1983]; Müller [1981]; Müller and Zenk [1983]). Mooring positions and the major features of bottom topography are shown in Fig. 1, and a summary of the depths and durations of individual records are presented in Table 1. Only data from Aanderaa Current Meters were used to ensure a consistent data set, and only records with a minimum length of 4 months were selected to allow the use of ordinary harmonic analysis to resolve M_2, S_2, K_1 tides and inertial signals (Godin [1972]). The vertical profiles of Brunt-Väisälä-frequency N required for the modal analysis were obtained from Price [1983] who had presented density distributions from historic hydrographic data averaged in 10° × 10° squares.

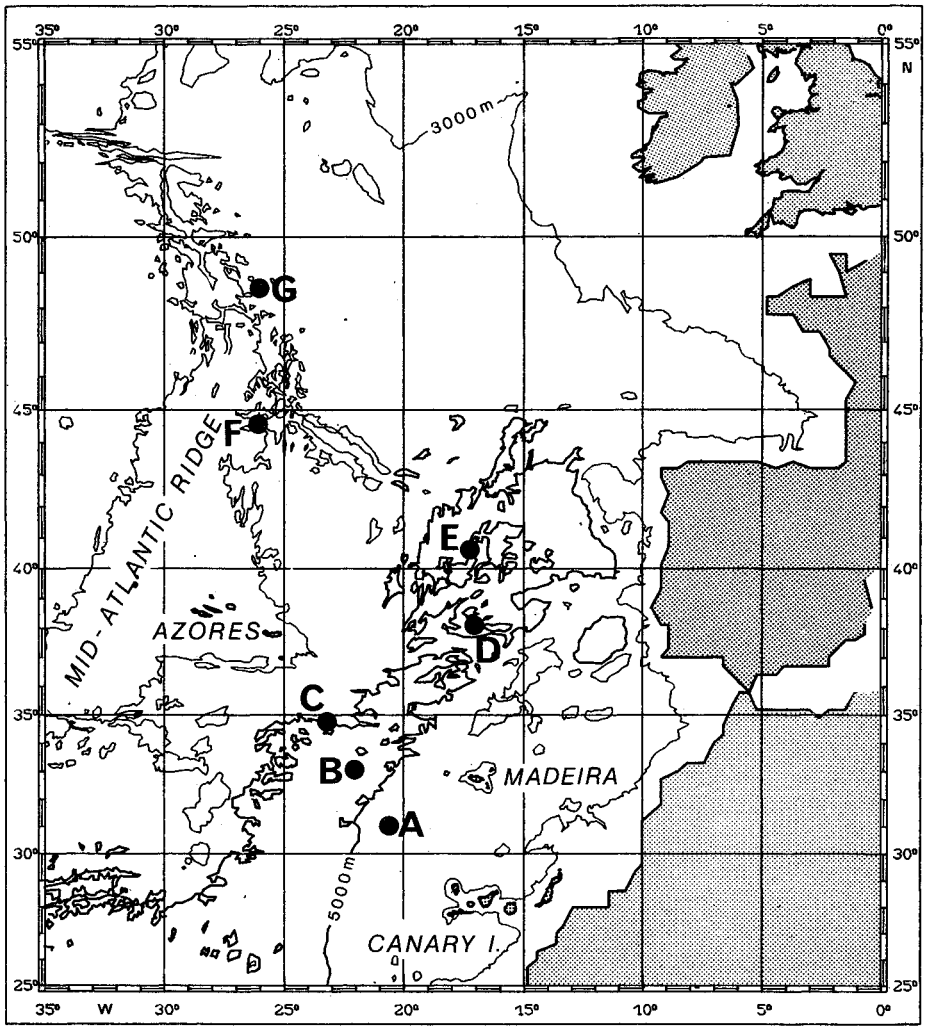

Fig. 1. Topographic map with positions A to G of moorings, depth lines indicating 3000 m and 5000 m levels

Table 1

Depths and observation periods of moored current meter records used

nominal position and depth	year: 1977 1978 1979 1980 1981 1982 1983
A 31° N 20° W NEADS site 12 4850 m	IfM no: 278 203 524 705 1139 2974 4692
B 33° N 22° W NEADS site 1 5260 m	IfM no: 184 264 276 276-2 276-3 125 196 245 379 499 428 673 632 703 755 629 935 1004 1160 1032 1585 1608 1535 3089 3008 3020 4770 4794
C 34° N 23° W NEADS site 11 5155 m	IfM no: 277-2 277-3 255 277 549 535 1192 1140 1663 1640 3029 3090 4722
D 38° N 17° W NEADS site 2 5550 m	IfM no. 203 229 242 780 796 1692 1466 3195 3210 3098 4224 4138 5079
E 40° N 17° W NEADS site 2,5 5310 m	IfM no: 230 485 2945 4050
F 44° N 26° W 3167 m	IfM no: 266 199 806 2497
G 48° N 26° W 3730 m	IfM no: 265-1 265-2 184 389 426 794 830 2515 2521

3 Methods of analysis

The area of investigation is north of the critical latitude where, according to linear internal wave theory, no diurnal baroclinic waves should exist. This is not so for semi-diurnal internal waves. Modal analysis was therefore applied in the case of semi-diurnal tides, discriminating between barotropic and low order baroclinic waves, while a vertical averaging scheme was selected for the study of diurnal barotropic tides. The method used for semi-diurnal components is summarized in the diagram of Fig. 2.

Normalized modes are calculated by numerically integrating the internal wave equation

$$\frac{d^2W}{dz^2} + \frac{N^2}{g}\frac{dW}{dz} + \frac{N^2 - \omega^2}{\omega^2 - f^2}\,\varkappa^2 W = 0$$

for the given Brunt-Väisälä-frequency N, using the Runge-Kutta method, with vertical velocity amplitude W, vertical coordinate z, gravitational acceleration g, angular frequency ω and horizontal wave number $\varkappa$. Vertical velocity equals zero at the surface and the bottom. The horizontal velocities can be obtained from the vertical derivative of the vertical velocity for each mode (Krauss [1966]). The Fourier coefficients of horizontal tidal currents, determined by harmonic analysis of the current meter time series, can then be least-squares approximated by a set of modes. The zero-order mode is equated to the barotropic tide. As an example, the modes of the M_2 tide resulting from our analysis are presented in Fig. 3.

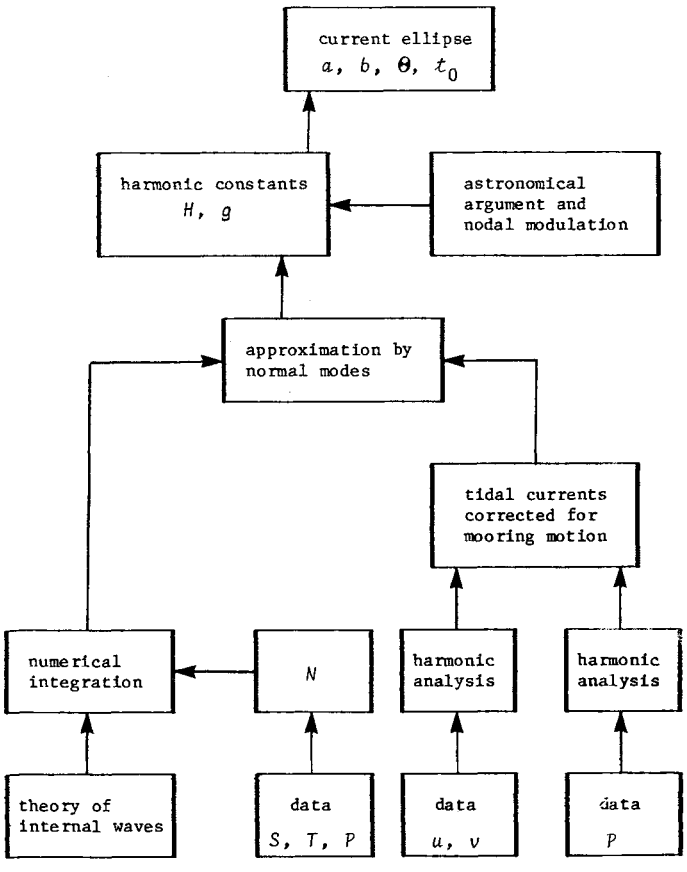

Fig. 2. Method of semi-diurnal tide analysis

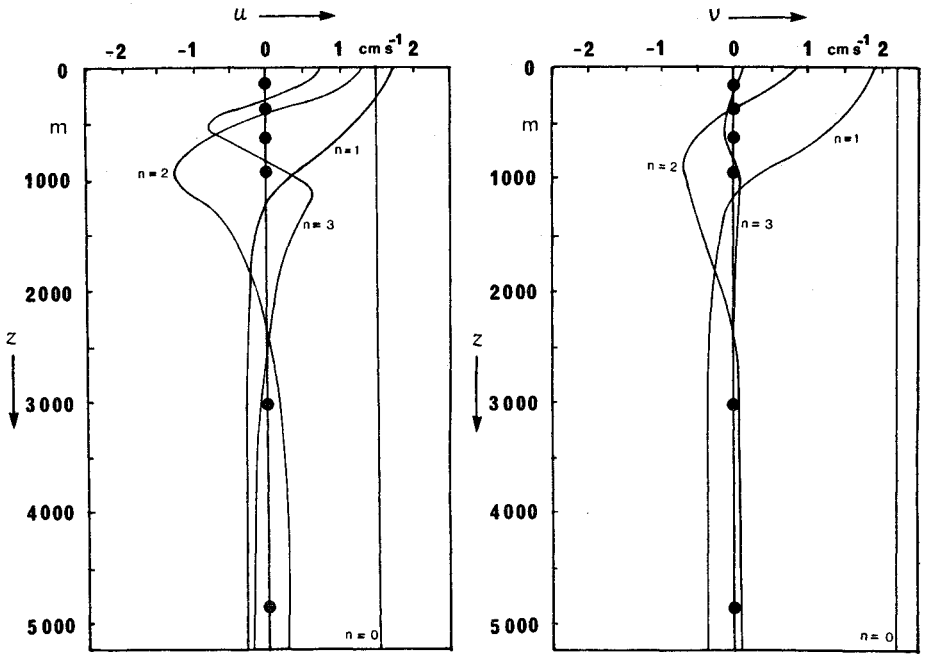

Fig. 3. Normal modes of the east (u) and north (v) component of the M_2 tide at position B, mooring no. 264-1.
Full circles indicate levels of current meters used for determining modal amplitudes

Mooring motions can not be neglected when determining the tidal currents, and typical errors due to this effect will be discussed here. The moorings usually contained pressure sensors near the top, and their records can be used to determine the changes in instrument depths due to the drag forces of currents acting on the mooring. With a current of a single period alone, the pressure will change with half that period. If superimposed on slower varying and stronger currents, the tidal period will be found in the pressure record. The pressure spectra contain strong semi-diurnal tidal peaks, indicating the latter conditions. According to Fofonoff [1966], resonant modes of deep-sea mooring motions will have periods which are several orders of magnitude below tidal periods. The response of the pendulum mode of a mooring to changing tidal current drag will therefore be almost in phase with the forcing current. The data indicate a decrease of instrument depth changes with increasing depth, suggesting a rigid inverted pendulum mode as a useful approximation. Assuming the mooring to move in the plane of the major tidal ellipse, the 180° phase uncertainty in relating pressure and current records can be removed. The procedure is included in the schematic diagram of Fig. 2, and results for one mooring will be presented later.

Phases are referred to Greenwich Mean Time (GMT) [Universal Time Co-ordinated (UTC)]. From the amplitude and phase information for the east and north components, tidal current ellipses can be determined, with the major axis $2a$, the minor axis $2b$, the angle θ of the major axis with respect to north, and the time t_0 of the current maximum referred to Greenwich (Doodson [1941]).

4 Tidal currents

Results from the M_2 analysis are presented in Fig. 4 and Tables 2, 3 and 4. Results from mooring 264-1 (B in Fig. 1) will be used to discuss the accuracy of the M_2 tidal parameters. The modal structure and the resulting partition of energy in those modes will depend on the actual profile of the Brunt-Väisälä frequency N. In Table 2 we compare results obtained when using the Price [1983] mean N profile and when using N calculated from a single CTD-profile obtained near the site of 264-1 in April 1982. Although deviations in the barotropic current component amplitudes are only 3 to 4%, the energy partition is affected considerably, with a change of about 7% in the barotropic tidal energy. The effect of mooring motion is presented in Table 3. Here, deviations in the current component amplitudes are of order 10%, while the partition of energy in modes is less affected.

Additional errors will be due to the deviations between actual tidal currents and the Gaussian fit using a limited number of normal modes. Due to different numbers of instruments on the moorings, the quality of the fit varies. Results for moorings 264-1 (B) and 242-1 (D) are given in Table 4. The deviations are in the range of 6 to 22% of current component amplitudes. Resulting errors are up to 15% for the major ellipse axis and up to 70% for the minor axis. In the case of narrow ellipses the sense of rotation becomes uncertain.

We will now discuss the results of the M_2 tide. According to Table 5, a strong dominance of mode 0 is usually found, and mode 1 clearly dominates among the baroclinic modes. In two cases, however, the energy of the first-order mode is larger than the energy of the barotropic mode (moorings no. 229-1 and 230-1). These two moorings were in place at the same time in late 1978, both to the north of the Azores Fracture Zone (D and E in Fig. 1). One might speculate that bottom topography in that area was responsible for the generation of baroclinic tides and an increased transfer of energy from barotropic to baroclines waves. Harmonic constants and tidal ellipse parameters for the barotropic M_2 tide are given in Table 6, and the ellipses (excluding moorings no. 229-1 and 230-1) are compared to the results obtained by Cartwright et al. [1980] and Saunders [1983] in Fig. 4.

At positions in the Northern Canary Basin, to the southeast of the Azores (A, B and C), we find the major axes of the current ellipses oriented towards the northeast, with clockwise rotation. While the major axis orientation is similar to that in the Iberian Basin, to the east of the Azores (D), anti-clockwise motion is found there. At the two positions north of the Azores Rise (F and G) the major axes are oriented approximately east-west, with anti-clockwise rotation. The trend in the regional variation of the major axis orientation is consistent with the results of Cartwright et al. [1980] and Saunders [1983], but major axis amplitudes differ up to about 30%. The differences between the results of this study and Saunders' [1983] much higher values at position B (NEADS Site 1) are particularly noteworthy.

It will be attempted to differentiate between progressive and standing tidal waves by inter-comparing our current phases with the phases of surface elevation from the Cartwright et al. [1980] observations. In the case of progressive waves, current and surface elevation should be in phase, while standing waves will result in a 90° phase shift. Sager [1963] proposed a classification of tides by allowing a deviation $\pm 1/16$ of a period from the in-phase or the out-of-phase condition to define progressive or standing waves, respectively, with all other waves being of mixed type. Cotidal lines and corange lines taken from Cartwright et al. [1980] are included in Fig. 4. When interpolating linearly between cotidal lines and directly comparing the phase information of the coastal gauges given in the figure with the phase data obtained here from current meter data (standard deviation ± 0.4 h) progressive waves are found in most cases. Only at site G is a mixed-type M_2 wave determined.

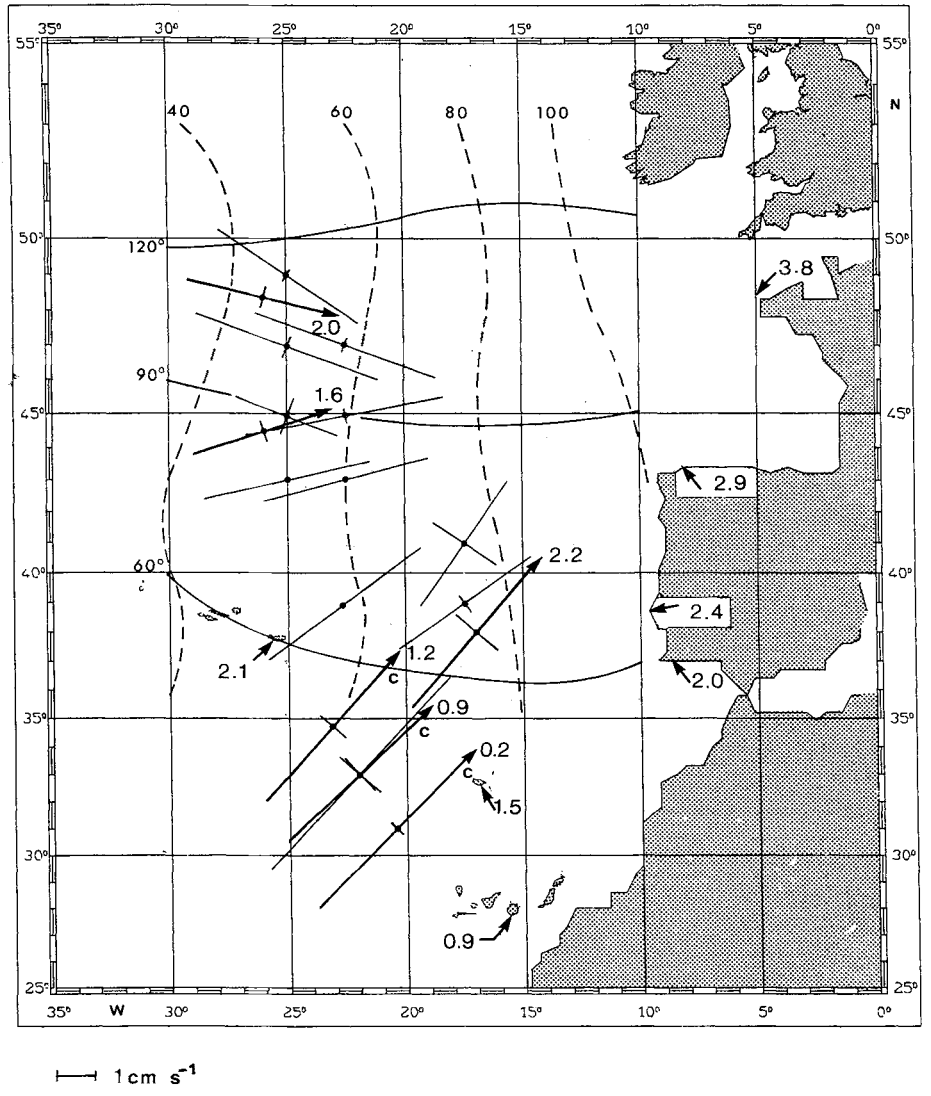

Fig. 4. M_2 tidal ellipses from this study (heavy lines) with *c* denoting clockwise rotation and from Cartwright et al. [1980] and Saunders [1983] (narrow line). Phase values of moored data and coastal data give hours referred to equilibrium tide maximum at Greenwich. Cotidal lines (solid) and corange lines (broken, in millibar) were taken from Cartwright et al. [1980]

Table 2

M_2 tidal ellipse data and energy partition on modes for Brunt-Väisälä frequency $\bar{N}$ obtained from mean density data and N^* from density data of one individual CTD station at the site (Mooring no. 264-1 (Site B)). East velocity component u, north velocity component v, major ellipse axis $2a$, minor axis $2b$, angle θ counted clockwise between north and major axis, and phase t_o with respect to equilibrium tide maximum at Greenwich. Negative sign of b denotes clockwise rotation

		Harmonic constants		Tidal ellipse			
		H	g	a	b	θ	t_o
		cm s^{-1}		cm s^{-1}	cm s^{-1}		h
$\bar{N}$	u:	1.5	29.2°	2.6	−0.2	34.5°	0.8
	v:	2.2	22.1°				
N^*	u:	1.5	23.5°	2.6	−0.0	36.5°	0.8
	v:	2.1	23.2°				

	Kinetic energy partition			
	Mode 0	Mode 1	Mode 2	Mode 3
$\bar{N}$	76.9%	16.9%	4.8%	1.4%
N^*	83.0%	12.5%	3.2%	1.3%

Table 3

M_2 ellipse data and energy partition with mooring motion considered (Mooring no. 264-1 (Site B)), and deviations from respective data for $\bar{N}$ in Table 2. For symbols see Table 2

		Harmonic constants		Tidal ellipse			
		H	g	a	b	θ	t_o
		cm s^{-1}		cm s^{-1}	cm s^{-1}		h
values and deviations	u:	1.3(+0.2)	40.7°(−11.5°)	2.4(+0.2)	−0.3(+0.1)	33.2°(+1.3°)	1.1(−0.3)
	v:	2.0(+0.2)	26.6°(−4.5°)				

	Kinetic energy partition			
	Mode 0	Mode 1	Mode 2	Mode 3
$\bar{N}$	74.2%	18.9%	5.7%	1.2%

Table 4

M_2 ellipse data for two selected moorings and deviations between actual M_2 tidal currents and Gaussian fit using modes 0 to 3. For symbols see Table 2

Identification		Harmonic constants		Tidal ellipse			
		H	g	a	b	θ	t_o
		cm s^{-1}		cm s^{-1}	cm s^{-1}		h
264-1	*u:*	1.5 ± 0.3	29.2° ±12.0°				
				2.6	−0.2	34.5°	0.8
(Site B)				±0.4	±0.1	±8.8°	±0.4
	v:	2.2 ± 0.5	22.1° ± 12.3°				
242-1	*u:*	2.3 ± 0.1	34.9° ±6.8°				
				3.2	1.5	38.2°	2.3
(Site D)				±0.2	±0.8	±4.0°	±0.1
	v:	2.6 ± 0.1	87.1° ± 5.2°				

Table 5

Energy partition on modes for M_2 tide

Identification		Kinetic energy partition				Number of depths
		Mode 0	Mode 1	Mode 2	Mode 3	
Site A	278-1	95.5%	3.4%	0.7%	0.4%	6
Site B	184-1	93.7%	6.2%	0.1%	—	4
	264-1	76.9%	16.9%	4.8%	1.4%	6
	276-1	78.9%	18.2%	0.1%	2.8%	6
	276-2	90.8%	9.0%	0.2%	—	5
	276-3	77.5%	16.1%	6.4%	—	5
Site C	277-2	64.0%	29.3%	4.2%	2.5%	6
	277-3	72.3%	26.9%	0.8%	—	5
Site D	203-1	71.5%	28.5%	0.0%	—	4
	229-1	46.4%	53.6%	—	—	3
	242-1	66.4%	33.6%	—	—	3
Site E	230-1	32.7%	67.3%	—	—	3
Site F	266-2	81.0%	19.0%	—	—	3
Site G	265-2	85.5%	14.5%	—	—	3

Table 6

Harmonic constants and tidal ellipse parameters for barotropic M_2 tide. For symbols see Table 2

Identification			Harmonic constants		Tidal ellipse			
			H	g	a	b	θ	t_o
			cm s^{-1}		cm s^{-1}	cm s^{-1}		h
Site A	278-2	*u:*	2.0	11.6°	2.8	−0.2	43.6°	0.2
		v:	2.1	2.9°				
Site B	184-1	*u:*	1.2	36.0°	1.7	−0.1	46.4°	0.8
		v:	1.2	19.7°				
	264-1	*u:*	1.5	29.2°	2.6	−0.2	34.5°	0.8
		v:	2.2	22.1°				
	276-1	*u:*	2.2	63.1°	2.7	−1.1	52.2°	1.6
		v:	1.9	17.5°				
	276-2	*u:*	2.0	29.2°	2.8	−0.7	45.5°	0.5
		v:	2.0	0.5°				
	276-3	*u:*	2.5	41.3°	3.0	−1.0	52.4°	0.9
		v:	2.0	1.6°				
Site C	277-2	*u:*	1.5	39.8°	2.2	−0.3	42.8°	1.1
		v:	1.6	26.5°				
	277-3	*u:*	2.0	51.7°	3.0	−0.8	38.9°	1.2
		v:	2.4	22.1°				
Site D	203-1	*u:*	1.3	55.8°	1.9	0.2	40.8°	2.1
		v:	1.5	66.0°				
	229-1	*u:*	1.2	343.2°	1.2	0.1	75.2°	11.9
		v:	0.3	7.9°				
	242-1	*u:*	2.3	34.9°	3.2	1.5	38.2°	2.3
		v:	2.7	87.1°				
Site E	230-1	*u:*	0.7	344.9°	0.8	0.4	68.1°	12.3
		v:	0.4	44.2°				
Site F	266-2	*u:*	1.8	42.1°	1.9	0.3	71.4°	1.6
		v:	0.7	72.1°				
Site G	265-2	*u:*	2.0	60.0°	2.0	0.3	103.9°	2.0
		v:	0.5	210.9°				

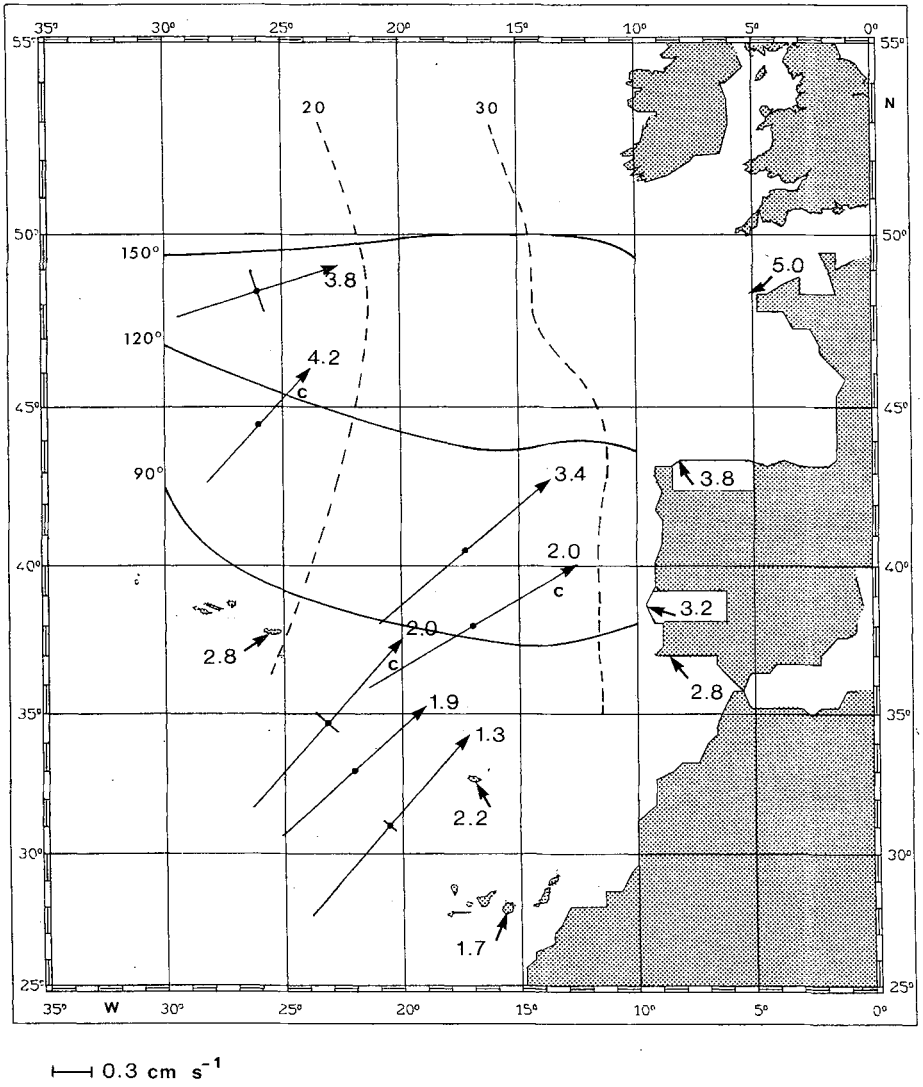

Fig. 5. S_2 tidal ellipses from this study with *c* denoting clockwise rotation. Phase values of moored data and coastal data give hours referred to equilibrium tide maximum at Greenwich. Cotidal lines (solid) and corange lines (broken, in millibar) were taken from Cartwright et al. [1980]

Results for the S_2 tide are given in Fig. 5 and Tables 7 and 8. Due to lower amplitudes compared to M_2, the relative errors are larger here, and the sense of rotation is therefore uncertain in this case. Except for mooring 229-1, the zero-order mode dominates. Ellipses are oriented towards the northeast throughout the area. No current ellipse data from earlier analyses are available for comparison of S_2. Within the accuracy available here (± 0.3 h) all waves are found to be progressive.

As explained earlier, a vertical averaging scheme was used for determining diurnal barotropic tides. Results for K_1 are presented in Fig. 6. Major axis orientation varies considerably. Progressive waves are found here except for site A where a mixed type of tide is determined. Because of large relative errors due to small amplitudes, O_1 tides will not be considered in this study. We conclude that the analysis provides tidal current information that can be used for the testing of numerical models of the M_2, S_2 and K_1 tide in the Northeast Atlantic. Deviations are found from the results of Cartwright et al. [1980] and Saunders [1983] with respect to M_2 tidal current amplitudes, but a similar current pattern is obtained.

Table 7

Energy partition on modes for S_2 tide

Identification		Kinetic energy partition			
		Mode 0	Mode 1	Mode 2	Mode 3
Site A	278-2	87.9%	10.7%	1.1%	0.3%
Site B	184-1	88.6%	11.4%	0.0%	—
	264-1	49.3%	14.7%	28.6%	7.4%
	276-1	84.5%	13.2%	0.1%	2.2%
	276-2	91.9%	8.0%	0.1%	—
	276-3	47.8%	41.9%	10.3%	—
Site C	277-2	91.9%	1.4%	4.9%	1.8%
	277-3	95.8%	3.7%	0.5%	—
Site D	203-1	86.5%	13.5%	0.0%	—
	229-1	42.0%	58.0%	—	—
	242-1	65.8%	34.2%	—	—
Site E	230-1	67.6%	32.4%	—	—
Site F	266-2	74.7%	25.3%	—	—
Site G	265-2	57.7%	42.3%	—	—

Table 8

Harmonic constants and tidal ellipse parameters for barotropic S_2 tide. For symbols see Table 2

Identification			Harmonic constants		Tidal ellipse			
			H	g	a	b	θ	t_o
			cm s^{-1}		cm s^{-1}	cm s^{-1}		h
Site A	278-2	*u:*	0.6	34.3°	0.9	0.0	40.1°	1.3
		v:	0.7	39.9°				
Site B	184-1	*u:*	0.5	57.4°	0.6	0.0	52.3°	2.0
		v:	0.4	63.0°				
	264-1	*u:*	0.5	61.6°	0.6	−0.0	56.0°	2.1
		v:	0.3	61.0°				
	276-1	*u:*	0.5	41.0°	0.7	0.3	37.3°	2.3
		v:	0.6	84.3°				
	276-2	*u:*	0.6	52.5°	0.8	−0.0	46.2°	1.7
		v:	0.6	51.4°				
	276-3	*u:*	0.7	71.2°	0.8	−0.3	48.0°	1.7
		v:	0.6	25.0°				
Site C	277-2	*u:*	0.6	58.5°	0.8	−0.1	49.2°	1.8
		v:	0.6	45.5°				
	277-3	*u:*	0.5	78.5°	0.9	−0.1	33.6°	2.2
		v:	0.7	39.9°				
Site D	203-1	*u:*	0.5	75.7°	0.8	0.1	41.1°	2.9
		v:	0.6	96.5°				
	229-1	*u:*	0.4	51.9°	0.5	0.2	58.4°	2.1
		v:	0.3	91.3°				
	242-1	*u:*	1.5	55.7°	1.5	−0.5	79.8°	1.7
		v:	0.6	347.9°				
Site E	230-1	*u:*	0.6	100.7°	0.9	0.0	48.6°	3.4
		v:	0.6	101.8°				
Site F	266-2	*u:*	0.4	129.6°	0.6	−0.0	40.7°	4.2
		v:	0.5	125.0°				
Site G	265-2	*u:*	0.6	107.7°	0.6	0.2	71.5°	3.8
		v:	0.3	153.5°				

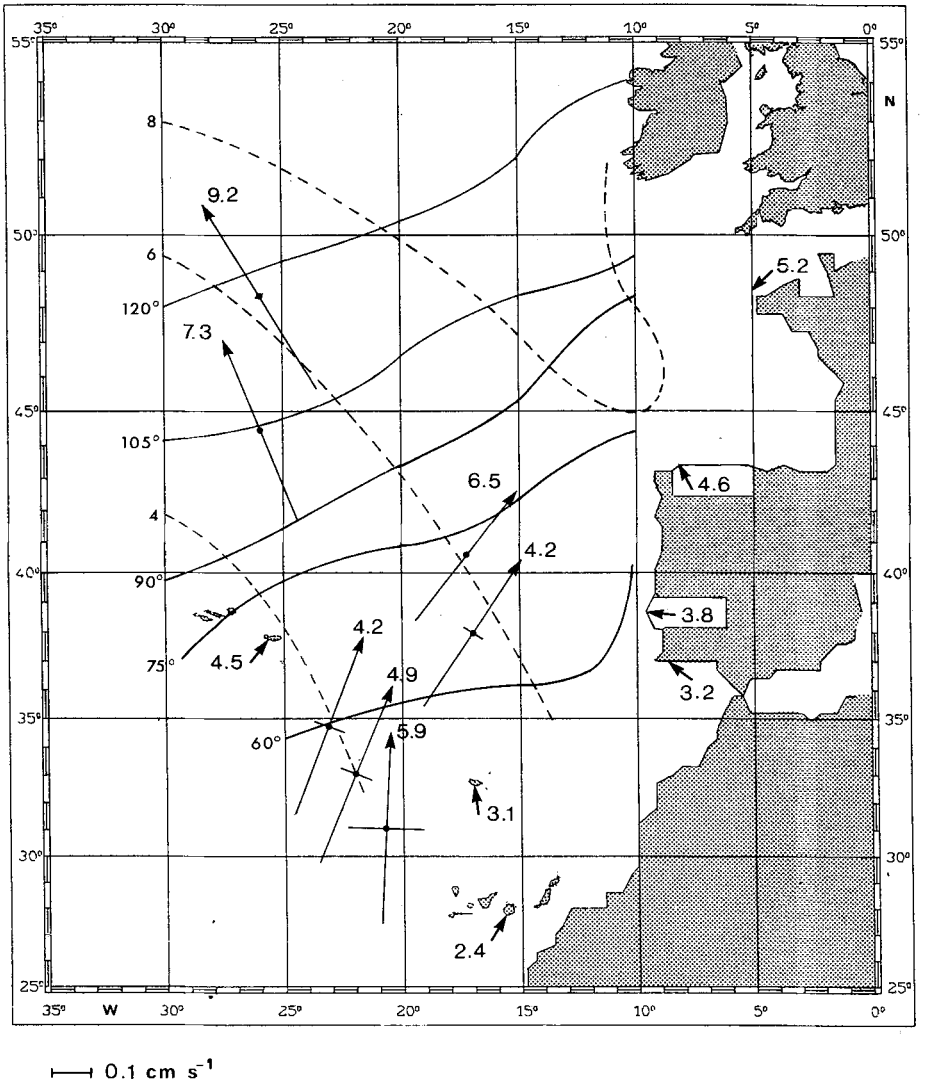

Fig. 6. K_1 tidal ellipses from this study with counter-clockwise rotation. Phase values of moored data and coastal data give hours referred to equilibrium tide maximum at Greenwich. Cotidal lines (solid) and corange lines (broken, in millibar) were taken from Cartwright et al. [1980]

Acknowledgements

The authors have benefited from discussions with Hartmut Peters on this subject. The study was partly funded by the Deutsche Forschungsgemeinschaft, Bonn.

References

Accad, Y. and C. L. Pekeris, 1978: Solution of the tidal equations for the M_2 and S_2 tides in the World Oceans from a knowledge of the tidal potential alone. Philos. Trans. Roy. Soc. (A) **290**, 235–266.

Baker, D. J., 1981: Ocean instruments and experiment design. In: Warren, B. A. and C. Wunsch (eds.), Evolution of physical oceanography. Cambridge, Mass.: MIT Pr. pp. 396–433.

Cartwright, D. E., A. C. Edden, R. Spencer et al., 1980: The tides of the Northeast Atlantic Ocean. Philos. Trans. Roy. Soc. (A) **298**, 87–139.

Dickson, R. R., 1983: Global summaries and intercomparisons: Flow statistics from long-term current meter moorings. In: Robinson, A. R.: Eddies in marine science. Berlin [usw.]: Springer. pp. 278–353.

Doodson, A. T., 1941: Admiralty manual of tides. London: His Majesty's Stationary Office.

Fofonoff, N. P., 1966: Oscillation modes of a deep-sea mooring. Geo-mar. Technol. **2**, 13–17.

Godin, G., 1972: The analysis of tides. Liverpool: Liverpool University Press. 264 pp.

Gould, W. J. and W. D. McKee, 1973: Vertical structure of semi-diurnal tidal currents in the Bay of Biscay. Nature. **244**, No. 5411, 88–91.

Hendershott, M. C., 1977: Numerical models of ocean tides. In: Goldberg, E. D., I. N. McCave, J. J. O'Brien et al. (eds.), The sea. Vol. 6: Marine modeling. New York: Wiley. pp. 47–95.

Hendershott, M. C., 1981: Long waves and ocean tides. In: Warren, B. A. and C. Wunsch (eds.): Evolution of physical oceanography. Cambridge, Mass.: MIT Pr. pp. 292–341.

Krauss, W., 1966: Methoden und Ergebnisse der theoretischen Ozeanographie. Band 2: Interne Wellen. Stuttgart: Borntraeger. 248 pp.

Meincke, J., G. Siedler and W. Zenk, 1975: Some current observations near the continental slope off Portugal. "Meteor" Forsch.-Ergebn. (A) No. 16, 15–22.

Müller, T. J., 1981: Current and temperature measurements in the North-East Atlantic during NEADS. Ber. Inst. Meeresk. Kiel. No. 90, 100 pp.

Müller, T. J. and W. Zenk, 1983: Some Eulerian current measurements and XBT-stations from the North East Atlantic, October 1980 – March 1982 – A data report. Ber. Inst. Meeresk. Kiel. No. 114, 145 pp.

Munk, W. H. and D. E. Cartwright, 1966: Tidal spectroscopy and prediction. Philos. Trans. Roy. Soc. (A) **259**, 533–581.

Price, J. M., 1983: Historic hydrographic and meteorological data from the North Atlantic and some derived quantities. Ber. Inst. Meeresk. Kiel. No. 117, 91 pp.

Regal, R. and C. Wunsch, 1973: M_2 tidal currents in the western North Atlantic. Deep-Sea Res. **20**, 493–502.

Sager, G., 1963: Atlas der Elemente des Tidenhubes und der Gezeitenströme für Nordsee, Kanal und Irische See. Rostock: Deutsche Akademie der Wissenschaften zu Berlin, Inst. Meeresk. 59 pp.

Saunders, P. M., 1983: Benthic observations on the Madeira Abyssal Plain: Currents and dispersion. J. Phys. Oceanogr. **13**, 1416–1429.

Schott, F., 1977: On the energetics of baroclinic tides in the North Atlantic. Ann. Geophys. **33**, 41–62.

Schwiderski, E. W., 1980: On charting global ocean tides. Rev. Geophys. Space Phys. **18**, 243–268.

Unesco, 1975: An intercomparison of open sea tidal pressure sensors. Report of SCOR working group 27: "Tides of the open sea." UNESCO Techn. Pap. Mar. Sci. No. 21, 67 pp.

Eingegangen am 7. März 1985

Angenommen am 18. März 1985

Anschrift der Verfasser:
Dipl. Oz. Gerhard Dick, Dr. Gerold Siedler
Institut für Meereskunde an der Universität Kiel, Düsternbrooker Weg 20, 2300 Kiel 1